

PETROGRAPHICAL AND GEOCHEMICAL INVESTIGATIONS OF STANNERN GROUP EUCRITES.

Devin R. McQuaig¹, Justin I. Simon², David W. Mittlefehldt², Rosalind M.G. Armytage³, ¹Dept. of Earth and Atmospheric Sciences, University of Houston (drmcquaig@uh.edu), ²ARES, NASA-JSC, ³Jacobs/JETS, NASA-JSC

Introduction: The howardite-eucrite-diogenite (HED) clan of meteorites represents a suite of mafic to ultramafic igneous rocks and breccias of them. They are linked together by O-isotope compositions [e.g., 1] and likely originate from the differentiated asteroid, 4 Vesta [2]. Radiogenic chronometers point to magmatic differentiation on the HED parent occurring within <10 Ma of solar system formation [3, 4], with the Ar-Ar record showing a more extensive history of impact heating [5]. As such, these basaltic eucrites display diverse igneous to metamorphic textures engendered by endogenous crustal processes and impacts [2, 6, 7]. They have fine to medium-grained textures with mineralogy dominantly consisting of plagioclase, pigeonite, and augite with minor to accessory phases including spinel, ilmenite, silica, troilite, Ca-phosphates, olivine, and Ni-poor metal [2].

Chemically, basaltic eucrites are divided into subgroups which are typically separated based on their Mg# (=100*molar Mg/(Fe+Mg)), Ti abundance, and incompatible trace element (ITE) abundances [2, 8]. Of these groups, the Stannern group (SG) eucrites are enriched in ITEs relative to the more abundant main group (MG) despite yielding similar Mg#s (42-35) [2, 3, 8, 9].

The purpose of this study is to constrain the petrogenesis of basaltic eucrites to better understand crustal evolution on early-formed planetary bodies. To achieve this, we conducted a detailed comparative investigation of the petrology and geochemistry of representative MG and SG samples.

Samples and Methods: This study is part of a collaborative project investigating MG and SG eucrites, including GRO 95533 and HOW 88401 (both MG), and LEW 88010, PCA 82501 and PCA 91179 (all SG). Here, our primary focus was on samples GRO 95533, PCA 91179 and HOW 88401. Our typical protocol was analysis of a thin section of each sample using optical microscopy, X-ray mapping using a scanning electron microscope (SEM), and determination of mineral phase composition using electron microprobe analysis (EPMA).

Results: General Petrography. Within this section, only eucrites containing potassium feldspar (K-spar) confirmed by EPMA, will be discussed. Our section of GRO 95533 has a discrete internal boundary separating distinct textural domains. The same phases are present in both domains, but they exhibit textural and chemical differences. We will refer to one domain as GRO 95533 N, and the other as GRO 95533 S.

Main group GRO 95533 (N & S) and HOW 88401 eucrites display sub-ophitic to ophitic magmatic

textures, but also exhibit evidence for subsolidus mineral growth and have areas of fragmental texture. Pyroxene grains exhibit exsolution of high-Ca pyroxene from low-Ca pyroxene with lamellae of variable widths, thinning as grains transition from core pigeonite to rim augite.

Plagioclase grains range from anhedral to nearly euhedral in GRO 95533 N, whereas they are anhedral to subhedral in HOW 88401 and GRO 95533 S. In all samples Carlsbad and albite twinning are prevalent, but on a few grains no twinning is visible. Patchy zoning of plagioclase was found in GRO 95533 N with interior areas of grains more sodic (blue in Fig 1) and inclusion-free, while some rims are more calcic (green in Fig 1) and inclusion rich.

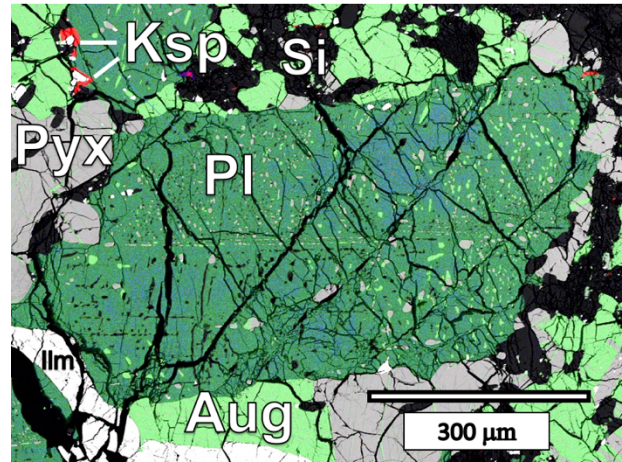


Figure 1. False color RGB X-ray map of a plagioclase grain in GRO 95533 N with patchy zoning. Aug: augite, Ilm: ilmenite, Ksp: K-spar, Pl: plagioclase, Pyx: low-Ca pyroxene, Sil: silica; Red = K, Green = Ca, Blue = Na.

Oxides are found throughout each sample with a higher abundance of ilmenite than chromite. Silica is disseminated throughout both eucrites with higher abundances in GRO 95533 N and larger grain sizes in HOW 88401 relative to the smaller grains and lower abundance in GRO 95533 S.

Rare K-spar grains populate areas associated with silica-rich mesostasis, silica intergrown with high-Ca pyroxene, along some fractures, and within plagioclase grains (Fig 1). These grains are less than ~10 μm and are not readily identifiable by optical microscopy but have been verified via EPMA.

Stannern group sample PCA 91179 is a brecciated monomict eucrite that displays sub-ophitic to ophitic texture and evidence for subsolidus mineral growth. It exhibits a finer overall texture than the other meteorites studied here. Like the MG samples its low-Ca pyroxenes

contain exsolved lamellae of high-Ca pyroxene. A few low-Ca pyroxenes are coarse, but the overall pyroxene sizes are very fine to medium.

Plagioclase grains are subhedral to anhedral with twinning being less common than in GRO 95533. However, plagioclase grains throughout PCA 91179 display patchy zoning as in GRO 95533 N (Fig 1).

Ilmenite is the most abundant oxide phase in PCA 91179, often sharing boundaries with spinel. However, overall oxide and sulfide phases are much less abundant in PCA 91179 than in the other eucrites we examined.

In PCA 91179 K-spar is more abundant than in our MG eucrites, though still rare, with two identifiable populations. Most is found in areas of mesostasis with high amounts of silica, high and low-Ca pyroxene, oxides, and phosphates. Other K-spar grains are found alongside or included within plagioclase grains.

Mineral Compositions: Pyroxenes. Pyroxene phases present in all samples are pigeonite and augite. Despite textural differences described between GRO 95533 S & N, the compositions of pyroxene phases are indistinguishable with Mg# 37 for the low-Ca pyroxene. Main group eucrite HOW 88401 has Mg# 39 and PCA 91179 has an Mg# 40. All of these are within the range of published MG & SG eucrites [e.g. 10].

Plagioclase. Of the MG eucrites studied here, HOW 88401 shows the widest variations with Ab₈₋₂₀. Texturally distinct GRO 95533 S & N also show different (though overlapping) ranges in their plagioclase composition with GRO 95533 S having Ab₉₋₁₃ and GRO 95533 N - Ab₁₁₋₂₀. The SG eucrite, PCA 91179, has a compositional range of plagioclase with Ab₁₂₋₂₁.

Oxides. Spinel and ilmenite are present in all samples. Spinel compositions have narrow ranges of 0.17 and 0.27 atoms per formula unit (apfu) in Al/Cr but wide ranges in mole% 2*Ti, varying from 7.86 to 43.03, as commonly observed for eucrites [2]. Every sample has ilmenite as the most abundant oxide phase. Ilmenites in all samples are homogenous with >93mole% FeTiO₃ component and minor amounts of MgO and MnO.

Potassium Feldspar. The K-spars identified in GRO 95533, HOW 88401, and PCA 91179 are nearly pure orthoclase, with Or_{>96} and all contain Ba as a minor component. Within GRO 95533 S, the K-spar has a BaO content of 0.34 wt%. In GRO 95533 N, the BaO content is 0.66 wt%. The BaO content of HOW 88401 is 1.45 wt%. The SG eucrite, PCA 91179, has the most abundant K-spar grains with an average BaO content of 1.49 wt%.

Discussion: The long-term goal of this project is to test the contamination by partial melts hypothesis of [9] for SG formation. Following the assimilation-fractional crystallization model of [11], a reasonable prediction of this hypothesis is that there could be trace element signatures in pyroxene and plagioclase indicating contamination of the SG magma during crystallization. Our petrologic work is establishing the background

needed for follow-on *in situ* trace element studies to test this hypothesis.

Our data are largely consistent with the observations reported in earlier eucrite studies, with the exception of the noted potassium feldspar occurrences. The K-spar in these eucrites are small, discrete grains, not exsolutions from hypersolvus feldspar. Their compositions have very low CaO, which is inconsistent with experiments [12]. There is limited mention in literature of the presence of potassium feldspar in basaltic eucrites [e.g., 9]. It has been identified in some clasts of Stannern group eucrite NWA 4523 [e.g. 9], but not for any MG sample. It is striking therefore, that it was found in at least half the samples, and in both MG and SG eucrites studied herein. Liquid immiscibility (LI) was proposed as an explanation for the generation of the K-spar in NWA 4523. Areas of “LI-produced” mesostasis, in which K-spar is surrounded by multiple phases: silica, pyroxenes, and plagioclase led [9] to suggest that the petrogenesis of the ITE rich SG was due to a partial melt of the MG contaminating the SG eucrite melt. The BaO contents of the K-spars of MG GRO 95533 N & S are much lower than the SG PCA 91179, and such, this is a possible interpretation for some observations. However, the BaO content of the MG HOW 88401 is as high as the SG PCA 91179, despite the K-spar occurring in similar textural settings as in GRO 95533, which might point to a different control on the Ba content rather than bulk ITE composition. The NWA 4523 study [9] did not include analyses of BaO for comparison.

It is likely that the patchy zoning of plagioclase grains, as shown in Figure 1, found in both GRO 95533 N (MG) and in multiple grains of PCA 91179 (SG) underwent an incomplete phase of equilibration. Whether these textures were produced before or after the K-spar (and generation of the mesostasis) is unclear. Future work will focus on *in situ* trace element studies of the various types and textures of feldspar in the suite of eucrites to further test their petrogenetic relationships.

References: [1] Scott E.R.D. et al. (2009) *GCA*, 73, 5835. [2] Mittlefehldt D.W. (2015) *Chemie der Erde-Geochemistry*, 75, 55. [3] Schiller M. et al. (2010) *GCA*, 74, 4844. [4] Touboul M. et al. (2015) *GCA*, 156, 106 [5] Bogard D. and Garrison D. (2003) *MAPS*, 38, 669. [6] Krot A.N. and Bizzarro M. (2009a) *GCA*, 73, 4919. [7] Yamaguchi A. et al. (1996) *Icarus*, 124, 97. [8] Stolper E. (1977) *GCA*, 41, 587. [9] Barrat J.A. et al. (2007) *GCA*, 71, 4108. [10] Takeda H. and Graham A.L. (1991) *MAPS*, 26, 129. [11] DePaolo D. J. (1981) *EPSL*, 53, 189. [12] Elkins L.T and Grove T.L. (1990) *Am Min.* 75, 5